Dispersion State of Zirconium Oxide Particles in Polymer Blends and Viscoelastic Behavior of the Composites

ARTICLE *in* NIHON REOROJI GAKKAISHI · JANUARY 2007

Impact Factor: 0.36 · DOI: 10.1678/rheology.35.1

5 AUTHORS, INCLUDING:

Hiroshi Jinnai
Tohoku University
234 PUBLICATIONS **4,238** CITATIONS

Nihon Reoroji Gakkaishi Vol.35, No.1, 1~9
(Journal of the Society of Rheology, Japan)

Article

Dispersion State of Zirconium Oxide Particles in Polymer Blends and Viscoelastic Behavior of the Composites

Masaoki TAKAHASHI*, Satoru OSAWA*, Hiroshi JINNAI*, Hideki YAMANE**, and Haruhisa SHIOMI***

*Department of Macromolecular Science and Engineering, Kyoto Institute of Technology, Matsugasaki, Sakyo-Ku, Kyoto 606-8585, Japan
**Center for Fiber and Textile Science Science, Kyoto Institute of Technology, Matsugasaki, Sakyo-Ku, Kyoto 606-8585, Japan
***Department of Chemistry and Materials Technology, Kyoto Institute of Technology, Matsugasaki, Sakyo-Ku, Kyoto 606-8585, Japan
(Received : May 16, 2006)

Zirconium oxide (ZrO_2) particles are dispersed in polystyrene (PS)/poly(butyl methacrylate) (PBMA) and PS/poly(methyl methacrylate) (PMMA) blend melts with bicontinuous structure. ZrO_2 particles enter exclusively into PBMA phase in PS/PBMA blend, while the particles exist in both phases in PS/PMMA blend. The main cause for the exclusive localization in PBMA phase is the lowest entropy loss of the most flexible PBMA chains among the three polymers due to adsorption onto ZrO_2 particles. In PBMA phase, spherical aggregates of ZrO_2 particles are formed at a concentration of 11 vol%, while ZrO_2 particles make linear arrays at 21 vol% and branches at 29 vol%. These arrays and branches give very high second-plateau in G' at low frequencies. In PS/PMMA blend melt, linear arrays and branches appear in both phases even at 4.4 vol%, and network structure is formed at 11 vol%. Due to the structural difference, the PS/PMMA/ZrO_2 composite gives much higher second-plateau than that of PS/PBMA/ZrO_2, when compared at the same vol% of ZrO_2. A peculiar network structure is observed in PS/ZrO_2 composite at a low concentration of 4.4 vol%. The low value of G' close to that of the matrix at intermediate frequencies with a small number of spherical aggregates indicates very weak adsorption of PS chains to ZrO_2 particles.
Key Words: Zirconium oxide / Dispersion state / Composite / Polymer blend / Bicontinuous structure

1. INTRODUCTION

To achieve required functional properties in dispersion systems, control of dispersion is most important. The dispersion control of ceramics, metal and nano-carbon particles in polymer matrices depends on the functional properties required. For electrical conductivity, thermal conductivity and improvement of mechanical properties, network formation of dispersed particles is very effective. However, favorable dispersion state is usually a uniform distribution of particles. In both cases, the particle-polymer interfacial energy and the entropy loss due to adsorption of polymer chains on the particle surface play crucial roles in the dispersion state.

In the present study, structure-rheology relationship is investigated for zirconium oxide (ZrO_2) particles filled polymer systems. ZrO_2 is one of the most studied ceramic materials. Pure ZrO_2 has a monoclinic crystal structure at room temperature and transforms into tetragonal and cubic structures at very high temperatures (1170 °C and 2370 °C, respectively). A different oxide such as yttrium oxide Y_2O_3, calcium oxide CaO or magnesium oxide MgO is added to ZrO_2 to stabilize the tetragonal and/or cubic phases for sintering and related temperature changes. Addition of Y_2O_3 around 3 mol% yields tetragonal zirconia polycrystal (TZP), a fine grained microstructure (less than 1 μm) with high strength, toughness, and flexibility. Fully stabilized ZrO_2 with 4 - 10 mol% of Y_2O_3 is used in oxygen sensors and fuel cell membranes because it has an ability to allow oxygen ions to move rather freely with increasing Y_2O_3 through the crystal structure at high temperatures (above 600 °C). In the present study, partially stabilized ZrO_2 with 3 mol% Y_2O_3 is used to investigate the structure-rheology relationship of the composites with polymers and polymer blends.

Dispersion of ceramics particles under phase separation of polymer blend is treated theoretically and verified experimentally by Tanaka *et al.*[1] A system considered is a composite sandwiched between glass-plates with a gap d, and

the composite is glass-beads (G) filled polymer blend (A/B) with the volume fraction ϕ_G, ϕ_A and ϕ_B, where $\phi_G + \phi_A + \phi_B = 1$. The free energy F of the system per unit volume is expressed by

$$F = 4\pi a^2\left(\gamma_A n_A + \gamma_B n_B\right) + \frac{1}{d}\left[\gamma_A\left(\phi_A + \frac{4}{3}\pi a^3 n_A\right) + \gamma_B\left(\phi_B + \frac{4}{3}\pi a^3 n_B\right)\right] + \sigma f(d) \quad (1)$$

Here, a is the radius of glass-bead, γ_i the interaction energy between glass-bead and i-phase (i = A or B), n_i the number density of glass-beads in i-phase, σ the interfacial tension between the polymers A/B, and *f(d)* is the area of interface A/B per unit volume. The first (two terms), middle (consisting of 4 terms) and final terms in Eq. (1) denote contributions from polymer-particle, polymer-plate and polymer-polymer interactions, respectively. Since the interface area S between polymer and glass plate is not known, S is approximately evaluated by S = volume/d as shown in the middle (4 terms) of Eq. (1). The apparent volume fraction of i-phase increases to $[\phi_i + (4/3)\pi a^3 n_i]$, because n_i glass-beads enter into i-phase. It should be noted here that the entropy term is not considered in Eq. (1). From the free energy consideration on Eq. (1) with a condition of $d > 2a$, it is concluded that glass-beads exclusively enter into a polymer phase having smaller interaction energy (more wettable phase) until the closest packing in its phase. It is also shown that the ordered structure of glass-beads inside the more wettable phase slows down the coarsening of the phase.

On the other hand, Wu *et al.*[2] emphasized the importance of entropic term (entropy penalty due to adsorption of polymer chains) for particle dispersion in polymer blends. They investigated exclusive localization of carbon black (CB) and vapor-grown carbon fibers (VGCF) in polymer blends. They found that the selective location of CB and VGCF in polymer blends does not always depend on the interaction energy but is governed largely by the flexibility of the polymer chains. More flexible polymer chains are adsorbed preferentially on the rough carbon surface with less decrease in entropy (less entropy penalty). The roughness of CB surface is 1.0 - 100 nm.[3,4] The ends of VGCF are rough within a range of 10 nm,[5,6] while the filament body of VGCF is rather smooth. Wu *et al.* concluded that a decisive factor for the exclusive localization of CB and VGCF is the glass transition temperature T_g of the matrix polymer.[2] CB and VGCF exclusively enter into the polymer with lower T_g with an exception of Nylon 6. It should be emphasized here that the localization of CB and VGCF are investigated under the condition of equal viscosity of the component polymers. The preferential adsorption of flexible polymer chains on the carbon surface[2] and heterogeneous distribution of carbon particles in polymer blends[7-9] result in very low percolation threshold in the blends.[2,7-9]

The objectives of the present study are: 1) to clarify the localization of ZrO_2 particles (with 3 mol% Y_2O_3) in blends of polystyrene (PS) / poly(n-butyl methacrylate) (PBMA) and PS / poly(methyl methacrylate) (PMMA), and 2) to clarify the structure-rheology relationships for the composites. As matrices, amorphous polymers are used to avoid epitaxial crystallization and migration of particles to amorphous region in crystalline polymers. The glass transition temperatures of PS, PBMA and PMMA are shown in Table I.[10] In Table I other possible factors such as polymer flexibility and polarity[10] are also summarized, which may affect the localization of ZrO_2 particles in the blend. The characteristic ratio C_∞[10] and the number of main chain atoms between entanglement points Z_e[11,12] are adopted as factors being associated with chain flexibility. Relations between dispersion state of ZrO_2 particles and these factors will be discussed in Results and Discussion section. It is considered that bicontinuous structure of polymer blend[13] will be the best template for a three dimensional network structure of ceramics particles, if exclusive localization of the particles is realized. The method of this dispersion control utilizing the bicontinuous structure of polymer blends may be very useful for the future development of functional composites, in which the functionality is realized through the percolation network[14-17] of the particles.

2. EXPERIMENTAL

2.1 Materials

In Table II, molecular weights and zero-shear viscosities η_0 of the component polymers used in the present study are summarized. The weight-average molecular weight M_w and

Table I. Glass transition temperature T_g,[10] characteristic ratio C_∞,[10] number of main chain atoms between entanglement points Z_e[11,12] and polarity $x^{(p)}$[10] of PS, PBMA and PMMA. Values for atactic PS and atactic PMMA are adopted, when tacticity can be specified.

Sample	T_g	C_∞	Z_e	$x^{(p)}$
PS	100	9.85	350	0.168
PBMA	20	7.85	170	0.158
PMMA	105	8.65	200	0.281

the polydispersity index M_w/M_n were obtained by GPC measurements, where M_n is the number-average molecular weight. The M_w of PBMA is calculated using the calibration curve for PS. The η_0 of the component polymers at 200 °C and 240 °C are also shown in Table II. Two polystyrenes with different M_w (PS1 and PS2) were used for blends, to match the η_0 of other component (PBMA and PMMA). Thus, two components in each blend (PS1/PBMA and PS2/PMMA) have comparable η_0 in the range of 160 °C - 200 °C (PS1/PBMA) and 190 °C - 240 °C (PS2/PMMA).

The partially-stabilized ZrO_2 particles with 3 mol% Y_2O_3, 3Y-E, manufactured by Tosoh Co., Ltd. were melt-blended with PS1/PBMA and PS2/PMMA blends. The average diameter, density and specific surface area of ZrO_2 particles are 0.27 μm, 6.05 g/cm^3 and 16 m^2/g, respectively. The composites were prepared by melt-blending using a kneader and a single-screw extruder. To obtain better dispersion of ZrO_2 particles, stearic acid (SA) and dibutyl phthalate (DBP) were added before melt-blending, with the weight ratio of ZrO_2:SA:DBP = 100:1:1.5. The condition of melt-blending is summarized in Table III. The blending temperatures of the composites were changed so that the viscosities of all the component polymers in both composites had similar values in each blending process. In order to prove that enough time of melt-blending was given for steady state of dispersion of ZrO_2 particles, 50 min blending in addition to 25 min blending in kneader was made for the PS2/PMMA/ ZrO_2 composite.

Table II. The weight-average molecular weight M_w, polydispersity index M_w/M_n, and the zero-shear viscosity η_0 of component polymers.

Sample	M_w	M_w/M_n	η_0/Pas	
			200°C	240°C
PS1	1.2×10^5	2.1	950	
PS2	2.0×10^5	2.4	6000	490
PBMA	2.3×10^5 *1	2.4	520	
PMMA	6.0×10^4	2.3	7400	270

*1 Using the calibration curve for PS

Table III. Conditions for melt-blending and melt-press.

Sample	Kneader	Single Screw Extruder	Melt Press
PS1/PBMA/ZrO_2	160 °C 15 rpm 25 min	180 °C 10 rpm	200 °C 3 MPa 18 min
PS2/PMMA/ZrO_2	190 °C 15 rpm 25, 50 min	220 °C 10 rpm	200 °C 3 MPa 18 min

2.2 Viscoelastic Measurements

Frequency dependences of the storage and loss moduli, $G'(\omega)$ and $G''(\omega)$, of the matrices and composites were measured using the Bohlin Stress Rheometer CSM with 25 mmϕ parallel plate geometry and 1 mm gap. The range of linear viscoelasticity was determined from the strain dependences of G' and G'' for each sample. A strain amplitude of 0.01 or 0.03 was given to the composites and the matrices with bicontinuous structure. The time dependences of G' and G'' were measured before frequency sweep to confirm the steady state.

2.3 SEM Observations

After viscoelastic measurement, each sample was quenched by liquid nitrogen, and the cross section of the sample was cut out at 2 mm from the edge. Polishing of the surface was not made for composite samples, because ZrO_2 particles came off with the matrix polymers by polishing. In case of a polymer blend without ZrO_2 particles, the surface was polished after etching PBMA phase by acetic acid (40 °C, 60 min) for PS1/PBMA or etching PS by cyclohexane (40 °C, 15 min) for PS2/PMMA. Platinum was vapor-deposited under vacuum with the thickness of several tens nm on the surface of the composite or polymer blend to observe dispersion state of ZrO_2 particles and/or phase separated structure of polymer blend by scanning electron microscope (SEM, KEYENCE VE-7800) and field emission type SEM (FE-SEM, Hitachi S-800).

3. RESULTS AND DISCUSSION

3.1 Structure and Viscoelasticity of PS1/PBMA Blend

First, we discuss about the structure-rheology relationship for the matrix, 50/50 (wt/wt) blend of PS1/PBMA. As shown in Fig. 1, this polymer blend has typical bicontinuous structure. The SEM micrograph of Fig. 1 was taken after dynamic viscoelastic measurement (after 60 min at 200 °C) and quenching by liquid nitrogen. Since the PBMA phase is etched off by acetic acid, only the PS1 phase can be seen. The frequency dependence data of storage and loss moduli, G' and G'', of PS1/PBMA blend are shown in Fig. 2 (bottom, as data for 0 vol% of ZrO_2). Due to the coarsening of bicontinuous structure of PS1/PBMA blend, G' and G'' of the blend melt decrease with time. In order to overcome this coarsening problem, all the low frequency data shown in Fig. 2 (PS1/PBMA and PS1/PBMA/ZrO_2) were obtained using new samples at each frequency. In Fig. 2, all the data (PS1/PBMA and PS1/PBMA/ZrO_2) are isochronal data (after 60 min at

200 °C). At low frequencies ($\omega \leq 0.40$ s^{-1}), G' and G'' of PS1/PBMA blend show a power law behavior

$$G' \sim G'' \sim \omega^n \quad (2)$$

with an exponent $n = 0.75$. This power law behavior is similar to that observed at the gel point in sol-gel transition of an end-linking polymer[14,15] and in a physical gelation of low molecular weight material[16,17]. If this power law holds in sufficiently wide range of frequency, the loss tangent $\tan\delta$ should satisfy a relation[14-17]

$$\tan\delta = \tan(n\pi/2) \quad (3)$$

From the two solid lines in Fig. 2 showing the power law behavior, we can see that $\tan\delta$ and $\tan(n\pi/2)$ of PS1/PBMA blend are 2.6 and 2.4, respectively. This suggests that the power law will fail at lower frequencies. The similarity in the power law behavior between polymer blends and gelation systems is considered to be only accidental, because bicontinuous structure of polymer blend is 3 dimensional network structure,[13] while percolation cluster at the gel point (threshold) is a precursor for a 3 dimensional network as its fractal dimension D at the threshold suggests, $D \cong 2.5$.[14-17] For polymer blends with bicontinuous structure (or with network structure), the power law behavior of the storage modulus, $G' \sim \omega^n$ with $0.5 < n \leq 1.0$, has been found experimentally in the frequency region of interface contribution.[18-21] The behavior similar to the percolation threshold, $G' \sim G'' \sim \omega^n$ with $\tan\delta = \tan(n\pi/2)$, was also observed[22]. However, these behaviors are somewhat vague due to the coarsening of bicontinuous structure during rheological measurement and to possible acceleration of domain growth (or break up) affected by small (or large) amplitude oscillation.

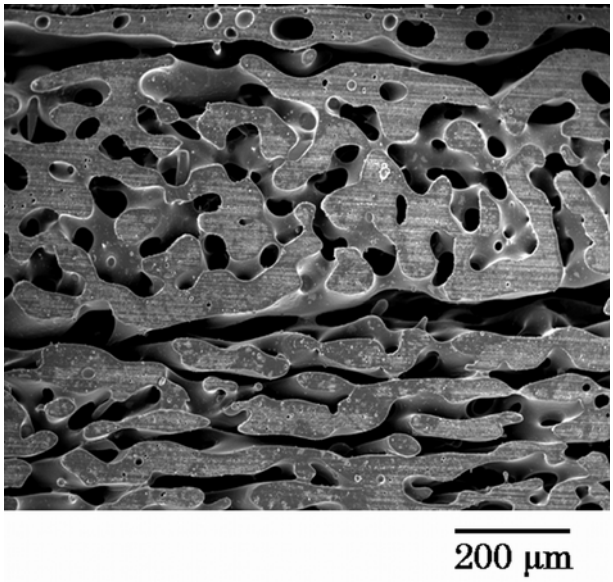

Fig. 1. SEM micrograph of a 50/50 blend of PS1/PBMA quenched from 200 °C after viscoelastic measurement. The PBMA phase is etched and only the PS1 phase is shown.

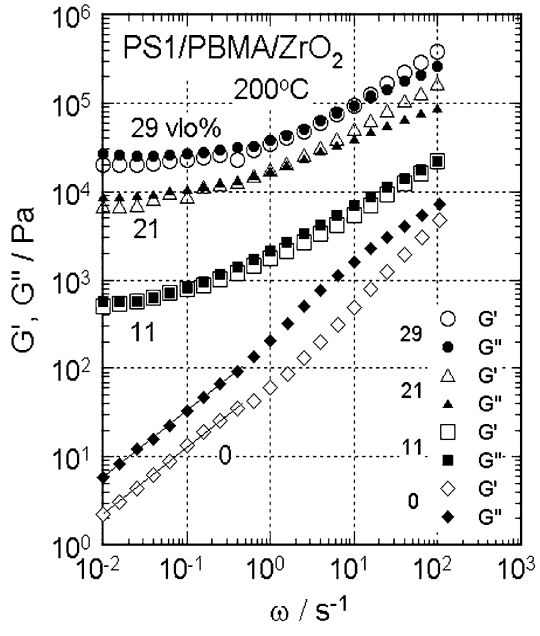

Fig. 2. Frequency dependences of the storage and loss moduli of PS1/PBMA/ZrO_2 composites and the matrix PS1/PBMA (50/50).

3.2 Structure and Viscoelasticity of PS1/PBMA/ZrO_2 Composites

Next, we discuss about the structure-rheology relationship for the PS1/PBMA/ZrO_2 composites. In a preliminary investigation, selective localization of ZrO_2 particles in PS1/PBMA blends is examined. SEM micrographs in Fig. 3 show dispersion state of ZrO_2 particles (11 vol%) in 30/70 (Fig. 3a), 50/50 (Fig. 3b) and 70/30 (Fig. 3c) blends of PS1/PBMA. Figure 3b was obtained after viscoelastic measurement (Fig. 2) by quenching the sample. Figures 3a and 3c were obtained using samples which experienced the same thermal and flow histories as those of the sample of Fig. 3b. In all SEM micrographs, ZrO_2 particles are exclusively localized in PBMA phase, which is the dominant phase in Fig. 3a but becomes the minor phase in Fig. 3c. Due to this exclusive localization, the apparent volume fraction of PBMA phase increases to *ca*. 60 % in 50/50 blend of PS1/PBMA. This apparent increase in the PBMA phase can clearly be seen in Fig. 3b.

In Table I, literature values for the matrix polymers (PS, PBMA and PMMA) are summarized which are considered to affect the compatibility of ZrO_2 particles with these polymers.

When the tacticity can be specified, values for atactic PS and atactic PMMA are adopted. Since the zero-shear viscosities of the component polymers are comparable in each blend, the effects of T_g on the mobility and monomeric friction coefficient[11] are minor. Both the characteristic ratio, C_∞, and the number of main chain atoms between entanglement points, Z_e, are associated with chain flexibility, although Z_e is also concerned with bulkiness of side chains and other factors, or the chain dimensions as a whole.[23] PBMA has the smallest values of C_∞ and Z_e, while PS has the largest values. From the C_∞ and Z_e values, PBMA is considered to be most flexible in these three kinds of polymers. The polarity $x^{(p)}$ of these polymers is also shown in Table I, which is evaluated from the polar component of surface tension or cohesive energy density.[10] The $x^{(p)}$ is the highest for PMMA and the lowest for PBMA, and is considered to have minor effect for adsorption and localization. It can be concluded that the main cause for the exclusive localization in PBMA phase is the lowest entropy loss of the most flexible PBMA chains due to adsorption onto ZrO_2 particles.

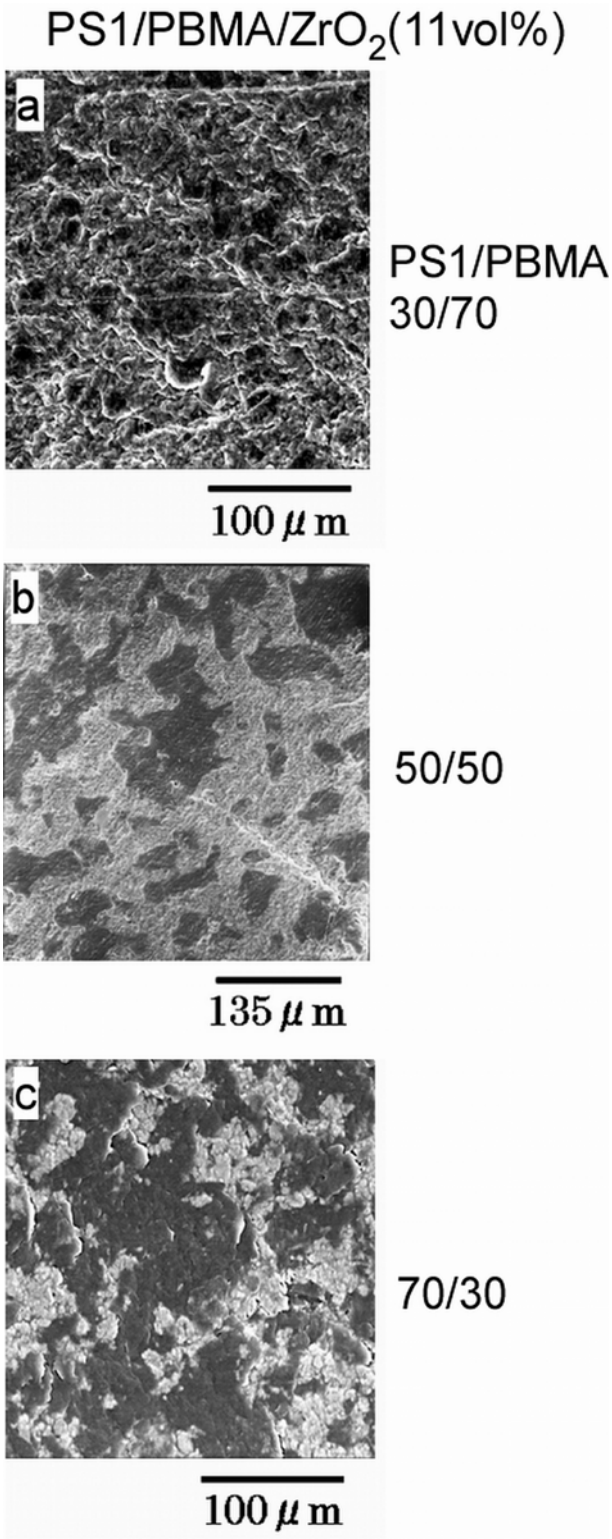

Fig. 3. SEM micrographs showing dispersion state of ZrO_2 particles (11vol%) in PS1/PBMA blends: a) 30/70, b) 50/50 and c) 70/30 blends.

In the composite samples, the coarsening of the bicontinuous structure of matrix polymer blends becomes slower with increasing ZrO_2 content. In our composite system, $\phi_{zirconia} \leq 29$ vol% $< \phi_{PBMA}$, and in principle, all ZrO_2 particles can enter exclusively into the PBMA phase. For high loading samples (21 and 29 vol% of ZrO_2 particles), the effect of coarsening on G' and G'' data has been found to be negligible when the viscoelastic data are obtained within 60 min. Figure 2 shows frequency dependences of G' and G'' of the composites, which are isochronal data after 60 min. Even at relatively low concentration of 11 vol% of ZrO_2, the composite gives high second plateau in G' at low frequencies. At intermediate and high frequencies, the composite also shows rather high values of G'. These results indicate selective adsorption of PBMA chains to the surface of ZrO_2 particles and effective cross-linking between the particles. The height of second plateau increases prominently for samples with 21 and 29 vol% of ZrO_2.

The dispersion state of ZrO_2 particles in bicontinuous PBMA phase observed by SEM is shown in Fig. 4. At 11 vol%, ZrO_2 particles form spherical aggregates in PBMA phase as shown in Fig. 4a. Each aggregate is composed of several ZrO_2 particles. Since emergence of linear array of ZrO_2 particles is very rare at 11 vol%, high second plateau at low frequencies and high G' at intermediate frequencies (Fig. 2) can be attributed to the effective cross-linking by adsorbed PBMA chains. Adsorbed PBMA chains, on the other hand, prevent ZrO_2 particles from gathering to form larger aggregates at 11 vol%. At higher concentrations such as 21 vol%, ZrO_2 particles make linear arrays (sometimes with short branches) in addition to spherical aggregates as shown in

Fig. 4b, while the particles form branches as well as linear arrays and spherical aggregates at 29 vol% in PBMA phase (Fig. 4c). These arrays and branches give very high second-plateau in G' at low frequencies. Smaller aggregates with adsorbed PBMA chains give high G' at intermediate frequencies.

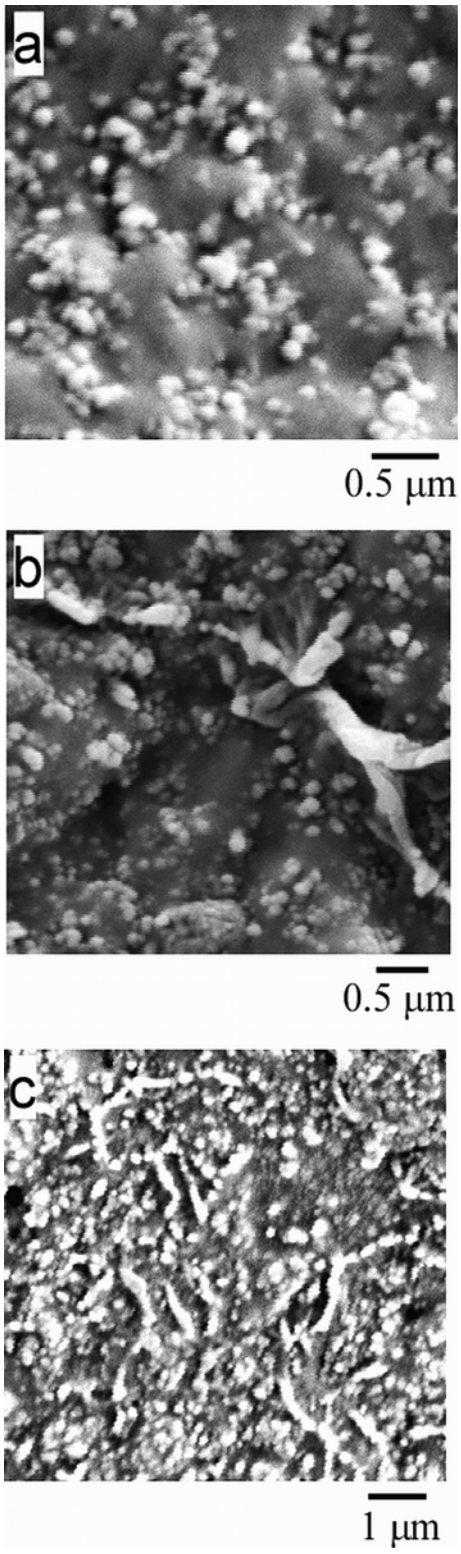

Fig. 4. SEM micrographs showing dispersion state of ZrO_2 particles in bicontinuous PBMA phase: a) 11 vol%, b) 21 vol%, c) 29 vol%.

As shown in Fig. 2, G'' at low frequencies, or in the frequency region of aggregate-structure contribution, is close to G'. This indicates that these aggregate structures are loosely connected structure composed of ZrO_2 particles with considerable energy loss.

3.3 Structure and Viscoelasticity of PS2/PMMA/ZrO_2 Composites

In Fig. 5 (bottom), frequency dependences of G' and G'' of the matrix, 50/50 blend of PS2/PMMA, at 240 °C are shown as data for 0 vol% of ZrO_2. All the G' and G'' data shown in Fig. 5 including those of the PS2/PMMA/ZrO_2 composites are isochronal data after 60 min. The coarsening of bicontinuous structure of the PS2/PMMA blend is prominent at 240 °C, but the power law behavior of G' and G'' can still be seen at $\omega \leq 0.63$ s^{-1}. The power law exponent n is obtained from the slope of the solid lines in Fig. 5 as $n = 0.83$. The loss tangent is $\tan\delta = 4.0$ while $\tan(n\pi/2)$ becomes 3.7. The same relation $\tan\delta > \tan(n\pi/2)$ is obtained for PS2/PMMA blend as in the case of PS1/PBMA blend. It has been found experimentally that the exponent n for G' increases with the process of coarsening and breakup of bicontinuous (or network) structure in polymer blends.[18-21)]

In Fig. 6, dispersion state of ZrO_2 particles in 50/50 blend of PS2/PMMA is shown for the concentration of 4.4 and 11 vol%. Selective localization of particles in one phase is not the case for the PS2/PMMA/ZrO_2 composites, where ZrO_2 particles exist in both phases. Basically, compatibility of PS/ZrO_2 and PMMA/ZrO_2 is not good due to the entropy penalty. From the C_∞ and Z_e values shown in Table I, PMMA chains

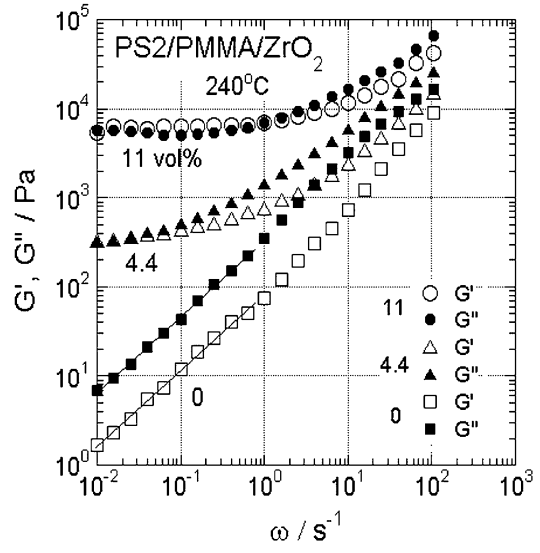

Fig. 5. Frequency dependences of the storage and loss moduli of PS2/PMMA/ZrO_2 composites and the matrix PS2/PMMA (50/50).

are considered to be more flexible than PS chains. Thus, PMMA chains are expected to have better compatibility with ZrO_2 particles due to smaller entropy loss. However, in PS2/PMMA blend no clear localization of ZrO_2 particles was found. Combination of PS (with the lowest flexibility) and PBMA (with the highest flexibility) is necessary for the exclusive localization. It should be noted here that much longer time for blending (50 min) in a kneader can not improve the compatibility in PS2/PMMA blend. Even at the concentration of 4.4 vol%, ZrO_2 particles form linear arrays and branches in addition to spherical aggregates in PS2 and PMMA phases as shown in Fig. 6a. At 11 vol% (Fig. 6b), branches and network structure of ZrO_2 particles are observed in both phases. Due to these branches and network structure, G' of the composites shows very high second plateau at low frequencies as clearly seen in Fig. 5. Compared at the same concentration (11 vol%), the second plateau is much higher for PS2/PMMA/ZrO_2 (Fig. 5) than for PS1/PBMA/ZrO_2 (Fig. 2). This difference is clearly attributed to the structural difference; branches and network structure in the former (Fig. 6b) and spherical aggregates in the latter (Fig. 4a).

To confirm lack of compatibility in PS2/ZrO_2 and PMMA/ZrO_2 systems, SEM observations and viscoelastic measurements were made for these single polymer component systems. SEM micrographs in Fig. 7 show dispersion state of 4.4 vol% ZrO_2 particles after viscoelastic measurement (after 60 min at 240 °C). In PS2, ZrO_2 particles make network structure or highly branched structure as shown in Fig. 7a. ZrO_2 particles also make branched structure in PMMA matrix (Fig. 7b), but there also appear spherical aggregates and linear arrays, suggesting somewhat better compatibility with PMMA. This better compatibility is attributed to smaller entropy loss of PMMA chains due to larger flexibility. From

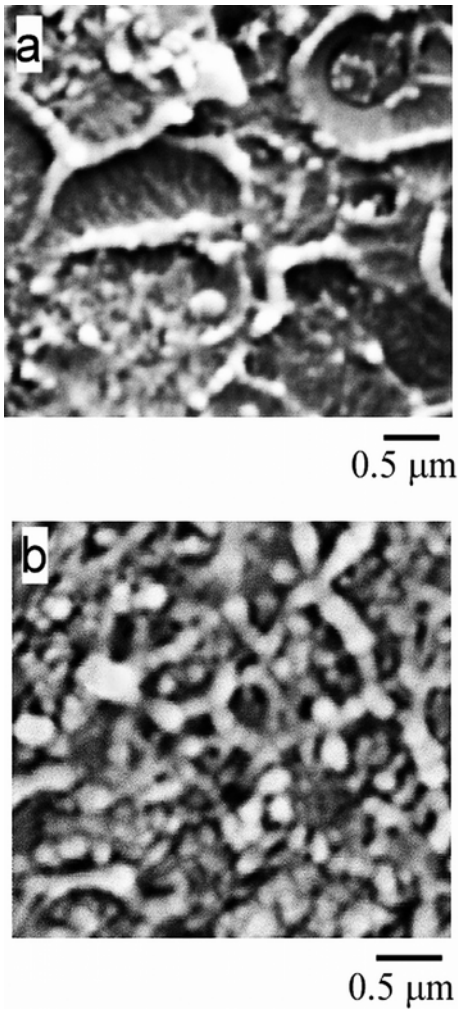

Fig. 6. SEM micrographs showing dispersion state of ZrO_2 particles in 50/50 blend of PS2/PMMA: a) 4.4 vol%, b) 11 vol%.

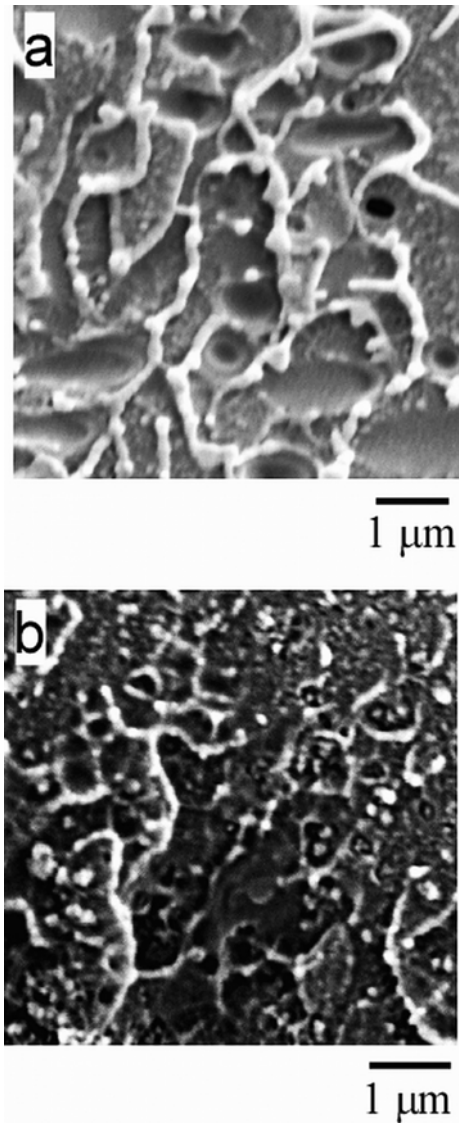

Fig. 7. SEM micrographs showing dispersion state of 4.4 vol% ZrO_2 particles: a) in PS2, b) in PMMA.

computer simulation based on a fluid particle dynamics method, Tanaka and Araki demonstrated that colloidal particles in viscous matrix make linear arrays and branched structure, when hydrodynamic interactions between the particles are taken into account.[24] The linear array (chainlike open structure) and branched structure predicted from this simulation are very similar to the observed structures shown in Figs. 7a and 7b. In Figs. 8 and 9, frequency dependences of G' and G'' for the composites PS2/ZrO_2 and PMMA/ZrO_2 with 4.4 vol% of ZrO_2 are shown, together with those for the matrices. The second plateau of both systems at the lowest frequency measured has comparable height, but G' behavior at intermediate frequencies is very different. In PS2/ZrO_2 system, the G' value around 1 $s^{-1} < \omega < 10$ s^{-1} is close to that of the matrix. On the other hand, in PMMA/ZrO_2 system the G' value in the corresponding frequency region is far above that of the matrix. It is considered that this difference in G' is due to the differences in the adsorption state of the matrix chains and the number of smaller aggregates. Stronger adsorption of PMMA chains to particles suppress the connectivity among particles, producing larger number of smaller aggregates and effective cross-linking between aggregates. Smaller aggregates with cross-linking by adsorbed PMMA chains result in higher G' at intermediate frequencies. On the other hand, much weaker adsorption of PS2 chains gives much smaller contribution to G' at intermediate frequencies. However, better connectivity of particles due to the weak adsorption of PS2 chains results in the comparable height of second plateau at low frequencies.

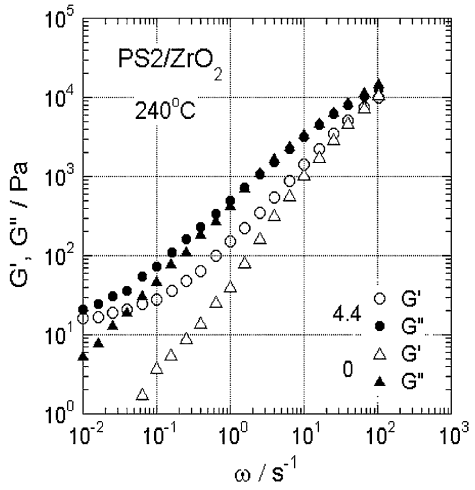

Fig. 8. Frequency dependences of the storage and loss moduli of PS2/ZrO_2(4.4 vol%) composite and the matrix PS2.

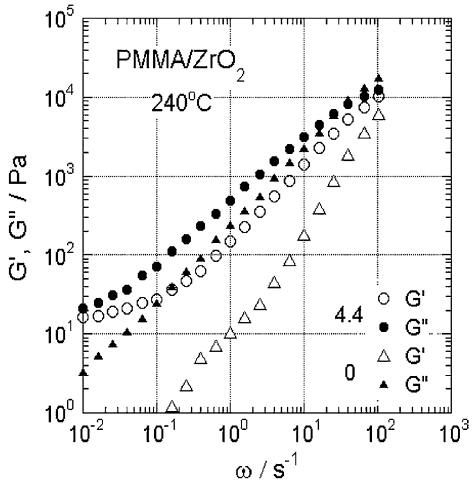

Fig. 9. Frequency dependences of the storage and loss moduli of PMMA/ZrO_2(4.4 vol%) composite and the matrix PMMA.

4. CONCLUSIONS

Dispersion state of zirconium oxide (ZrO_2) particles is investigated in blends of polystyrene (PS)/poly(butyl methacrylate) (PBMA) and PS/poly(methyl methacrylate) (PMMA) with bicontinuous structure. Exclusive localization of ZrO_2 particles in PBMA phase is found in PS1/PBMA blend. The main cause for the exclusive localization into PBMA phase is the lower entropy loss of more flexible PBMA chains than PS chains in adsorption onto ZrO_2 particles. In PBMA phase, ZrO_2 particles make spherical aggregates at 11 vol%. There appear linear arrays at 21 vol% and branch structure at 29 vol%. On the other hand, in PS2/PMMA blend, no apparent localization of ZrO_2 particles is found. In both phases, ZrO_2 particles form linear arrays and branches even at 4.4 vol%. At 11 vol%, branches and network structure are observed widely. Somewhat stronger adsorption of PMMA chains to ZrO_2 particles than that of PS chains is suggested from SEM observation and viscoelastic measurement of PS/ZrO_2 and PMMA/ZrO_2 systems. However, this difference in adsorption tendency does not affect the selective localization of ZrO_2 particles in PS2/PMMA blend.

Formation of spherical aggregates, linear arrays, branches and network structure makes the second plateau higher in this order. Adsorption of PBMA chains (and less importantly of PMMA chains) suppresses the connectivity of ZrO_2 particles, producing larger number of smaller aggregates such as spherical aggregates. The smaller aggregates with effective cross-linking by adsorbed polymer chains give very high values of G' at intermediate frequencies.

Acknowledgements

This work was partially supported by Grant-in-Aid for Scientific Research (B) No. 16350127 and 18350119 from the Japan Society for the Promotion of Science. We thank Tosoh Co., Ltd. and Tosoh Ceramics Co., Ltd. for supplying zirconia powder, 3Y-E, and PS and PBMA samples. A PMMA sample supplied by Sumitomo Chemical Co., Ltd. is also appreciated.

REFERENCES

1) Tanaka H, Lovinger AJ, Davis DD, *Phys Rev Lett*, **72**, 2581 (1994).
2) Wu G, Asai S, Sumita M, Yui H, *Macromolecules*, **35**, 945 (2002).
3) Donnet JB, Wang TK, *Macromol Symp*, **108**, 97 (1996).
4) Donnet JB, *Rubber Chem Technol*, **71**, 323 (1998).
5) Endo M, Takeuchi K, Kobori K, Takahashi K, Kroto HW, Sarkar A, *Carbon*, **33**, 873 (1995).
6) Darmstadt H, Roy C, Kaliaguine S, Ting JM, Alig RL, *Carbon*, **36**, 1183 (1998).
7) Wu G, Asai S, Sumita M, *Macromolecules*, **32**, 3534 (1999).
8) Wu G, Miura T, Asai S, Sumita M, *Polymer*, **42**, 3271 (2001).
9) Wu G, Asai S, Zhang C, Miura T, Sumita M, *J Appl Phys*, **88**, 1480 (2000).
10) Brandrup J, Immergut EH, Grulke EA, eds, *"Polymer Handbook"*, 4th ed, (1999), John Wiley, New York.
11) Ferry JD, *"Viscoelastic Properties of Polymers"*, 3rd ed, (1980), John Wiley, New York.
12) Wu S, *J Polym Sci, Polym Phys*, **27**, 723 (1989).
13) Jinnai H, Watashiba H, Kajihara T, Takahashi M, *J Chem Phys*, **119**, 7554 (2003).
14) Takahashi M, Yokoyama K, Masuda T, Takigawa T, *J Chem Phys*, **101**, 798 (1994).
15) Koike A, Nemoto N, Takahashi M, Osaki K, *Polymer*, **35**, 3005 (1994).
16) Takenaka M, Kobayashi T, Hashimoto T, Takahashi M, *Phys Rev E*, **65** 041401 (2002).
17) Takenaka M, Kobayashi T, Saijo K, Tanaka H, Iwase N, Hashimoto T, Takahashi M, *J Chem Phys*, **121**, 3323 (2004).
18) Polios IS, Soliman M, Lee C, Gido SP, Schmidt-Rohr K, Winter HH, *Macromolecules*, **30**, 4470 (1997).
19) Vinckier I, Laun HM, *Rheol Acta*, **38**, 274 (1999).
20) Vinckier I, Laun HM, *J Rheol*, **45**, 1373 (2001).
21) Zhang ZL, Zhang HD, Yang YL, Vinckier I, Laun HM, *Macromolecules*, **34**, 1416 (2001).
22) Castro M, Prochazka F, Carrot C, *J Rheol*, **49**, 149 (2005).
23) Fetters LJ, Lohse DJ, Richter D, Witten TA, Zirkel A, *Macromolecules*, **27**, 4639 (1994).
24) Tanaka H, Araki T, *Phys Rev Lett*, **85**, 1338 (2000).